Journal of Materials Chemistry B

ROYAL SOCIETY OF CHEMISTRY

PAPER



Cite this: *J. Mater. Chem. B*, 2023, **11**, 6428

# Thermo-responsive polymer-modified metal–organic frameworks as soft–rigid enzyme-reactors for enhancement of enzymolysis efficiency using a controllable embedding protocol†

Juan Qiao,‡[ab] Cheng Cheng,‡[ac] Dan Li[d] and Li Qi*[ab]

Received 16th April 2023,
Accepted 3rd June 2023

DOI: 10.1039/d3tb00844d

rsc.li/materials-b

Enzyme immobilization is a suitable strategy to promote biosensing, biocatalysis and the industrial applications of biomacromolecules. Although considerable efforts have been devoted to the construction of metal–organic frameworks (MOFs)-based porous nano-reactors, their enzymolysis efficiency cannot be tuned by varying the external conditions due to the fixed conformation of the encapsulated enzymes. In this work, a controllable embedding protocol was developed based on the concept of stimuli-responsive polymer modified MOFs. Using MOFs as a rigid template for thermo-responsive polymer modification and consequently utilizing the polymer–MOFs complexes for enzyme (glucose oxidase, horseradish peroxidase, trypsin, cytochrome *c*, glutaminase) immobilization, different porous nano-reactors were fabricated. Most importantly, the polymer on the MOF surface exhibited good ability to form a "soft nest" at high temperature for inducing the confinement effect and further improving the enzymolysis efficiencies of the nano-reactors 3.75–37.7-fold. Moreover, a colorimetric sensing method was developed to detect serum glucose with the proposed nano-reactors. This strategy is highly versatile and suitable for diverse rigid MOFs modified with stimuli-responsive soft-polymer-nests and enzymes.

## 1. Introduction

Enzymes, which are excellent natural catalysts, have fascinating properties, such as regio- and stereoselectivity and inherently high efficiency, allowing for their outstanding contribution in biotechnological applications.[1,2] However, some characteristics of enzymes, such as susceptibility to pH and temperature fluctuations, and low tolerance to inhibitors and most organic solvents, severely restrict the efficiency of enzymatic systems in practical applications. Enzyme immobilization is a promising strategy for improving their reusability and stability, ease of operation and continuous-flow production, which thereby promotes the industrialization of enzymes.[3–8] But, despite these merits, most matrices for immobilizing enzymes still have some limitations. Porous materials such as sol–gel matrices, hydrogels, organic particles and mesoporous silica have large surface areas and pore volumes, and are the commonly utilized materials for enzyme immobilization. However, these materials often suffer from enzyme-leaching, enzyme-denaturation and limited mass transfer, which greatly affect the biological activity of immobilized enzymes.[9–13]

Metal–organic frameworks (MOFs) are a type of porous material, which consist of metal nodes and organic linkers linked through coordination bonds. Compared with the traditional inorganic porous materials, MOFs combine the advantageous characteristics of uniform pore channels and versatile framework compositions.[14] In recent years, MOFs have been used as the protective network for enzyme immobilization in the areas of biosensing and biocatalysis.[15–18] There are four main methods for enzyme immobilization using MOFs as matrices: surface attachment, covalent linkage, pore encapsulation, and co-precipitation.[19–22] However, surface attachment and pore encapsulation often suffer from a low loading efficiency or high leaching rates due to the weak interactions between the MOFs and the enzymes or the mismatch of the MOF pore-size and the enzymes.[23] Tightly encapsulated enzymes within host MOFs *via* the co-precipitation method can make up for the above deficiencies, but enzymes confined in MOFs typically lack conformational

[a] *Beijing National Laboratory for Molecular Sciences, Key Laboratory of Analytical Chemistry for Living Biosystems, Institute of Chemistry, Chinese Academy of Sciences, Beijing 100190, China. E-mail: qili@iccas.ac.cn; Fax: (+86)10-62559373*
[b] *School of Chemical Sciences, University of Chinese Academy of Sciences, Beijing 100049, China*
[c] *College of Chemistry & Environmental Science, Hebei University, Baoding 071002, P. R. China*
[d] *College of Chemistry and Material Science, Jinan University, Guangzhou 510632, P. R. China*

† Electronic supplementary information (ESI) available. See DOI: https://doi.org/10.1039/d3tb00844d

‡ These authors contributed equally.

freedom, which may greatly affect substrate recognition.[24] Mass transfer of substrates and products can also be affected by the small pores in MOFs, and consequently the internally packed enzymes may have substantially reduced catalytic activity.[25,26]

Many approaches have been developed to obtain the optimal conformational freedom of the immobilized enzymes. MOFs based on coordination defects were constructed to facilitate substrate transport and greatly enhance the catalytic activity of the encapsulated enzymes.[27] A nano-reactor was prepared by combining enzyme activators and linkers encapsulation, resulting in improved biocatalytic activity.[28] A peptide-directed strategy was developed that enabled *in situ* tailoring of MOF-shrouded biohybrids into controllable nano-reactors and increased their catalytic activity.[29] Then, a double-layered nano-cage-based zeolite imidazole framework was fabricated to encapsulate enzymes, leading to good bioactivity and stability due to the dual confinement effect of the porous nano-reactors.[30] Although these methods have solved the problem of conformational freedom of immobilized enzymes to a certain extent, the residual activity of the immobilized enzymes is still limited.

Previous studies have proved that stimuli-responsive polymers are suitable for enzyme protection without loss of bioactivity. This makes stimuli-responsive polymers perfect ''soft nest'' templates for embedding enzymes. For example, pH-sensitive, temperature-sensitive and light-sensitive polymers have been applied for enzyme immobilization and the resulting nano-reactors enhanced the enzymolysis efficiency.[31–33] Combining the benefits of both soft stimuli-responsive polymers and the rigid frameworks of MOFs to form ''stimuli-responsive polymer–MOFs'' may provide an opportunity to greatly enhance their performance. Recently, the concept of polymer–MOFs complexes has received wide attention. For instance, a hybrid of MOFs and polyethersulfone was prepared,[34] which provided an improvement in the adsorption capacity of analytes in comparison to the original MOF powder. Moreover, a post-immobilization hydrophobic modification strategy was proposed by coating MOFs with polydimethylsiloxane (PDMS). The higher the surface hydrophobicity of the PDMS–MOF, the more the lipase fixed on MOF–PDMS,[35] which opened a way for straightforward and versatile fabrication of polymer–MOF complexes. However, stimuli-responsive polymer–MOF complexes have rarely been explored to immobilize enzymes for further enhancing their enzymolysis efficiency to date.

Herein, a typical temperature-sensitive polymer, poly(*N*-isopropyl-acrylamide) (PNIPAM), was selected as the adjustable moiety due to its unique manipulation *via* ''on-demand'' remote control as well as ''on–off'' switchable control by temperature. A versatile approach was developed to fabricate ''thermo-responsive polymer–MOF-based nano-reactors''. In this system, PNIPAM would provide a tailorable space to the immobilized enzymes and boost the catalytic activities of the nano-reactors. Firstly, the temperature-sensitive polymer was modified onto the MOF with dimethylvinyloxazolinone (VDMA) as the linker. The enzymes were then immobilized on the P(NIPAM-*co*-VDMA) chains to form polymer–MOF@enzymes-based nano-reactors. The catalytic activity of the nano-reactors at different temperatures was investigated. The principle based on soft PNIPAM chains forming a soft nest at high temperature, which maintained the conformational freedom of the immobilized enzymes and induced the confinement effect to promote the catalytic activities of the nano-reactors, was explored. Finally, a colorimetric sensing system for detection of glucose in real serum samples was constructed through a cascade reaction.

## 2. Experimental section

The details of chemicals, instruments and the enzymatic activities of different nano-reactors are described in the ESI.†

### 2.1. Preparation of MOFVN

P(NIPAM-*co*-VDMA)@UIO-66-$NH_2$ (MOFVN) was prepared through UV-initiated radical polymerization (Fig. S1, ESI†). 50.0 mg UIO-66-$NH_2$ was added to 1.4 mL dimethylvinyloxazolinone (VDMA) monomer (10.0 mmol) to form a stable dispersive system by ultrasound for 0.5 h at room temperature, and then the mixture was stirred overnight at room temperature. Then, 20.0 mL 1,4-dioxane containing 1.1131 g *N*-isopropyl acrylamide (NIPAM, 10.0 mmol) monomer and 20.0 mg of azodiisobutyronitrile (AIBN) was added into the above reactant. After three freeze–thaw cycles and degassing, the reaction flask was filled with nitrogen, and the reaction system was irradiated with an ultraviolet lamp (365 nm) for 24.0 h. At the end of the reaction, the solid obtained by centrifugation was washed with *N*,*N*-dimethylformamide (DMF) three times. The solid MOFVN was dried in a vacuum oven at 50 °C for 24.0 h.

### 2.2. Construction of enzymes@MOFVN

Immobilization of enzymes was achieved through the amide reaction between the lactone in MOFVN and the amino group residue on the enzymes (Fig. S2, ESI†). 5.0 mg of different enzymes (glucose oxidase, GOx; horseradish peroxidase, HRP; trypsin, TRY; cytochrome *c*, Cyt-*c*; glutaminase, Glnase; Table S1, ESI†) and 1.0 mg MOFVN were added to 2.0 mL PBS solution (pH 7.4), respectively. After agitating for 2.0 h at 4 °C, the product was collected by centrifugation at 10 000 rpm for 10.0 min and washed three times with PBS. Finally, 2.0 mL PBS was added for ultrasonic suspension and stored at 4 °C for later analysis.

## 3. Results and discussion

### 3.1. Preparation and characterization of MOFVN

First, the modification of P(VDMA) and P(NIPAM) onto the MOF was successfully conducted to form MOFVN. In this protocol, VDMA was selected as the multifunctional binding molecule. Its lactone group could react with $NH_2$ in the UIO-66-$NH_2$ MOF to form a covalent bond, which then provided the ethylene bond for NIPAM polymerization. Additionally, the lactone groups in P(VDMA) also provided the anchor for the immobilization of the enzymes (Fig. 1).

After incubation with UIO-66-$NH_2$ assisted by ultrasonication and stirring, the VDMA fully diffused into the nano-pore channels of UIO-66-$NH_2$ and immobilized on the MOF: the product is

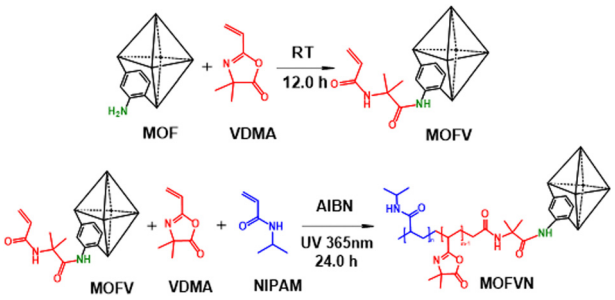


Fig. 1 Illustration of MOFVN preparation *via* UV-initiated radical polymerization.

named MOFV. Then, the grafting method was selected to add the fabricated sample to 1,4-dioxane and NIPAM monomer with AIBN as the initiator. This reaction was performed for 24.0 h under 365 nm UV irradiation. Consequently, the target product, UIO-66-$NH_2$ modified with P(VDMA-co-NIPAM (MOFVN) (Fig. 1), MOFVN was obtained by centrifugation and washed three times with DMF. The enzyme immobilization procedure is displayed in Fig. 2.

Fourier transform infrared (FT-IR) spectroscopy revealed a characteristic N–H stretching vibration peak at 3300 $cm^{-1}$ and C═O stretching vibration at 1660 $cm^{-1}$ (Fig. 3(A)). Powder X-ray diffraction (PXRD) (Fig. 3(B)) indicated that UIO-66-$NH_2$ has good crystallization and its crystal structure did not change after modification with P(VDMA) and P(NIPAM). The $^1$H nuclear magnetic resonance spectroscopy ($^1$H-NMR) spectra of UIO-66-$NH_2$, MOFV and MOFVN are shown in Fig. S1 (ESI†). Compared with UIO-66-$NH_2$, a chemical shift appeared at 1.4 ppm for MOFV with deuterium substituted for DMSO as the solvent. This is the characteristic chemical shift of the two methyl groups of VDMA. Additionally, a chemical shift at 1.1 ppm appeared in the $^1$H-NMR spectrum of MOFVN, which corresponded to the characteristic chemical shift of the methyl group of NIPAM. UIO-66-$NH_2$ was characterized by transmission electron microscopy (TEM) and the results are shown in Fig. 3(C), which showed that UIO-66-$NH_2$ had a typical octahedral shape and a size range from 150 nm to 200 nm. After modification with P(VDMA-co-NIPAM), TEM and scanning transmission electron microscopy (STEM) revealed an obvious polymer nest on the MOFVN surface (Fig. 3(D)). Notably, the polymer nest combined with the MOF tightly, which had no effect on the size of MOFVN. All the above characterizations

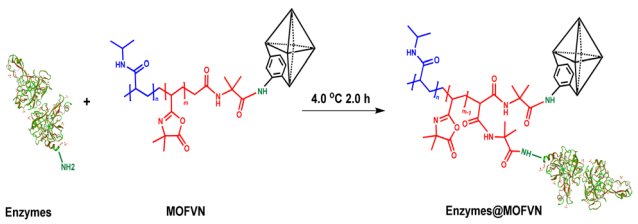


Fig. 2 Illustration of the enzyme immobilization procedure.

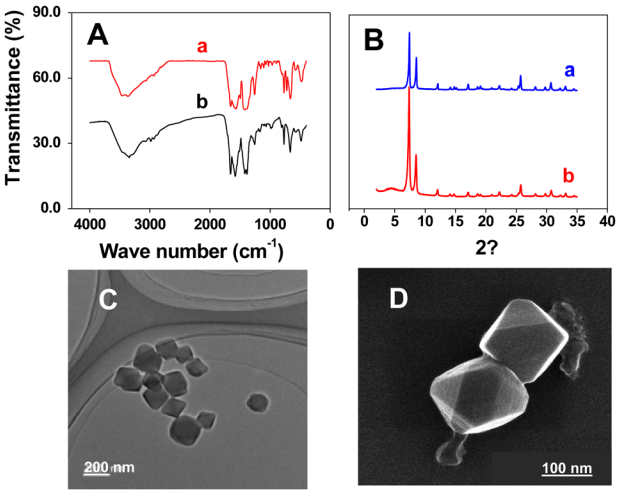


Fig. 3 (A) FT-IR spectra and (B) PXRD patterns of (a) the MOF and (b) MOFVN. TEM image of the MOF (C) and STEM image of MOFVN (D).

provided reliable structural information to inform subsequent experiments and confirmed the successful construction of polymer-coated UIO-66-$NH_2$.

### 3.2. Temperature-sensitive characteristics of MOFVN

The performance of MOFVN in response to temperature was explored using dynamic light scattering (DLS). The results showed that the particle size of MOFVN in aqueous solution increased from 247 nm to 275 nm with increasing temperature from 25 °C to 37 °C (Fig. S2, ESI†). Due to the destruction of hydrogen bonds in the thermo-sensitive polymer shell of MOFVN with the increase in temperature, the weakening of hydrophilic interactions and the dominance of hydrophobic polymer chain interactions resulted in the aggregation of the originally dispersed MOFVN particles and an overall increase in particle size. The results showed that the prepared MOFVN had good temperature sensitivity.

### 3.3. Construction of enzymes@MOFVN

The temperature-responsive enzymes@MOFVN-based nanoreactors were constructed. Five natural enzymes with different molecular weights were selected: GOx, Glnase, HRP, TRY and Cyt-*c*. Amides were generated through the lactone reaction of the amino acid residues in the enzymes with the unreacted VDMA in MOFVN (Table S1, ESI†). Fig. S3 (ESI†) shows the circular dichroism (CD) data of free HRP and the immobilized HRP, which indicated that there was no conformational change during the enzyme immobilization process. The schematic diagram of the enzyme immobilization process is shown in Fig. 2. To verify the success of enzyme immobilization, four enzymes in the nanoreactors were labeled with fluorescein isothiocyanate (FITC) with microwave assistance and the immobilization state of each nanoreactor was observed by confocal laser scanning microscopy (CLSM). Fig. 4(A)–(D) reveals that the signature fluorescence appeared in the nano-reactors. Fig. 4(E) describes the related catalytic activity of the different enzymes@MOFVN and enzymes@MOF. Almost no catalytic activity was detected for the

 

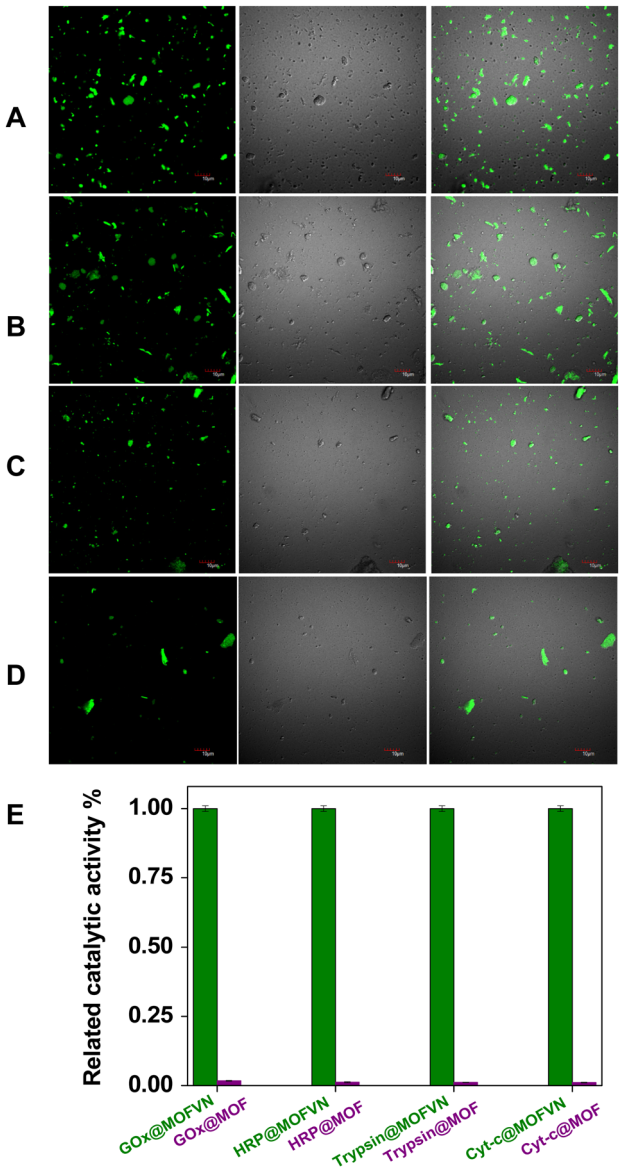


Fig. 4 CLSM images of the FITC labeled enzymes within the MOFVN ((A) GOx, (B) HRP, (C) TRY, (D) Cyt-*c*); excitation wavelength: 488 nm. (E) Related catalytic activity of different enzymes@MOFVN and enzymes@MOF.

enzymes@MOF, which was constructed by the incubation of enzymes with the MOF, that is, the enzymes were physically adsorbed onto the surface of the MOF. Notably, compared with enzymes@MOF, the enzymolysis efficiency of enzymes@MOFVN was much higher (Fig. 4(E)). These results indicated that enzymes@MOFVN was successfully prepared by chemically bonding the enzymes onto the polymer chains. Furthermore, the thermogravimetric analysis (TGA) of the MOF, MOFVN and enzymes@MOFVN showed that enzymes@MOFVN displayed the greatest weight loss (Fig. S4c, ESI†), while the weight loss of the MOF was the least (Fig. S4a, ESI†). These results indicated that the enzymes@MOFVN-based nano-reactors were successfully constructed.

To obtain the best enzyme immobilization efficiency, several key parameters were optimized using HRP as the reference (Fig. S5, ESI†). These included the proportion of block polymer synthesis, the proportion of the enzyme to MOFVN, and the HRP-immobilization duration. The optimization results showed that the optimal polymer synthesis ratio was 10.0 mmol : 10.0 mmol (Fig. S5A, ESI†), the ratio of HRP to MOFVN was 2.0 mg : 2.0 mg (Fig. S5B, ESI†), and the immobilization duration was 2.0 h (Fig. S5C, ESI†). Next, the amount of immobilized enzyme was determined by the Coomassie bright blue method. The linear relationship of Coomassie bright blue for detecting different enzyme immobilization concentrations is shown in Fig. S6 (ESI†). By measuring the amount of residual enzyme in the supernatant and calculating the difference from the total amount of enzyme, the amount of immobilized enzyme was obtained. The results are displayed in Table S2 (ESI†), which could be comparable to those of previously reported nano-reactors.

### 3.4. Mechanism of enzymolysis efficiency regulation

To evaluate the catalytic activity and temperature response performance of the constructed enzymes@MOFVN, the UV-vis colorimetric sensing assay and capillary electrophoresis technique were utilized. The enzymolysis efficiency of different nano-reactors was determined at 25 °C and 37 °C. Fig. 5 illustrates that the catalytic activity of enzymes@MOFVN was higher at 37 °C than at 25 °C, indicating that the thermo-responsive polymer in the nano-reactors played an important role in forming the "soft nest", inducing the confinement effect and boosting the enzymolysis efficiency.

The steady state of enzyme activity is usually described using classical Michaelis–Menten dynamics. The catalytic process of enzymes@MOFVN followed Michaelis–Menten behavior. Various nano-reactors including GOx@MOFVN (Fig. S7, ESI†), HRP@MOFVN (Fig. S8, ESI†), TRY@MOFVN (Fig. S9 and S10, ESI†), Cyt-*c*@MOFVN (Fig. S11, ESI†) and Glnase@MOFVN (Fig. S12 and S13, ESI†) were constructed. The substrates and the products of the enzymatic reactions were measured using the UV-vis adsorption method and CE technique (Fig. S9 and S12, ESI†). The relationship between the substrate concentration and initial reaction rate was investigated, and the Michaelis–Menten model was used to fit the experimental data (Fig. S7, S8, S10, S11 and S13, ESI†). The kinetic parameters of enzymes@MOFVN at 25 °C and 37 °C were calculated. The data are shown in Table 1.

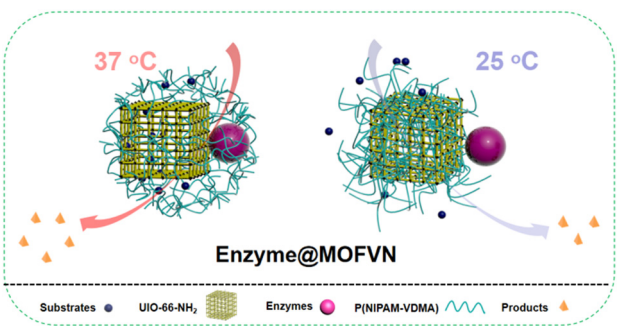


Fig. 5 Illustration of the thermo-responsive polymer effect on the catalytic activity of the enzymes@MOFVN-based nano-reactors at different temperatures.

Table 1 Kinetic parameters of different nano-reactors

| Nano-reactors | Temperature (°C) | $K_m$ (mM) | $V_{max}$ ($10^{-8}$ M $s^{-1}$) |
|---|---|---|---|
| GOx@MOFVN | 25 | 12.2 | 1.95 |
| | 37 | 1.15 | 0.24 |
| Glnase@MOFVN | 25 | 0.90 | 2.50 |
| | 37 | 28.0 | 10.0 |
| HRP@MOFVN | 25 | 0.04 | 1.34 |
| | 37 | 37.4 | 40.3 |
| TRY@MOFVN | 25 | 6.85 | 7.91 |
| | 37 | 9.72 | 298.1 |
| Cyt-*c*@MOFVN | 25 | 1.67 | 1.85 |
| | 37 | 0.36 | 1.55 |

Table 1 shows the kinetic analysis results. The kinetic parameters, apparent constants ($K_m$) and maximum Michaelis–Menten initial velocity ($V_{max}$) were obtained by fitting the Michaelis–Menten equation. Of the five nano-reactors, the catalytic activity of TRY@MOFVN, Glnase@MOFVN and HRP@MOFVN changed considerably with the temperature change. In comparison with the $V_{max}$ values obtained at 25 °C, their catalytic activities at 37 °C increased 37.7-fold, 3.75-fold and 30.1-fold, respectively. The $V_{max}$ value of Cyt-*c*@MOFVN was the same at the two temperatures. However, the $V_{max}$ of GOx@MOFVN decreased significantly. This was because the different molecular weights of the enzymes led to different states of MOFVN nano-frameworks. The three nano-reactors TRY@MOFVN, Glnase@-MOFVN and HRP@MOFVN showed greater catalytic activity improvement because, when the temperature increased, the polymer chains shrank, and consequently TRY (23.0 KD), Glnase (138.0 KD), HRP (43.0 KD) and substrates could be wrapped into a "soft nest". Therefore, an appropriate enzyme molecular weight (or an appropriate size) became the key factor for the construction of nano-reactors with suitable polymer density. In the soft polymer nest, the mass transfer distance from the substrates to the enzyme decreased, and the effective enzyme–substrate collisions increased. Additionally, other potential interference factors in the complex environment could be avoided. The lack of change in the catalytic activity of Cyt-*c*@MOFVN may have been due to the small molecular weight of Cyt-*c* at 13.0 KD, so the catalytic reaction space formed by the soft thermo-sensitive polymer and rigid MOF greatly restricted its conformational freedom, which in turn limited the substrate to approach the active site and to drop down its enzymolysis efficiency. In contrast to Cyt-*c*, for GOx, which has a high molecular weight (150.0 KD), the polymer chains were not enough to encapsulate the whole GOx@MOFVN, leading to the loss of the confinement effect and low enzymolysis efficiency, as shown in Fig. S14 (ESI†). Additionally, the stability and repeatability of the proposed nano-reactor were investigated to understand its usage performance. No significant decrease in catalytic activity within three weeks was observed when the nano-reactors were stored at 4 °C, while good recyclability of HRP@MOFVN is demonstrated in Fig. S15 (ESI†).

### 3.5. Serum glucose detection

A protocol for detecting glucose based on the GOx@MOFVN–HRP–TMB system was constructed. The UV-Vis absorption intensity related to the blue oxTMB product changed with the variation of glucose concentration. A good linear relationship was found between the UV-Vis absorption of oxTMB at 450 nm and glucose concentration, ranging from 10.0 to 100.0 μM (Fig. 6), with a regression equation of $y = 0.078$ [glucose] (μM) + 0.24 ($R^2$ = 0.997), and a limit of detection at 0.3 μM. This indicates that the developed colorimetric system is favourable for monitoring glucose in real biosamples.

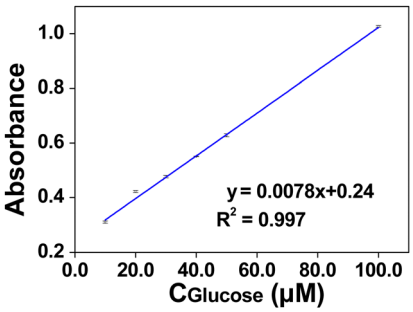


Fig. 6 Linear relationship between the UV-vis adsorption of oxTMB and glucose concentration.

The accuracy of the proposed assay was obtained by determining the recovery of standard glucose that was added into the rat serum samples. Table S3 (ESI†) displays the recovery data, which were in the range of 95.38–115.63% with RSDs < 2.35%, indicating the great potential of the proposed GOx@MOFVN–HRP–TMB system for accurate and highly sensitive detection of serum glucose.

## 4. Conclusions

Different thermo-sensitive polymer-modified MOF-based nano-reactors were successfully constructed by embedding five enzymes onto the polymer chains using a controllable protocol. With the polymer as the "soft nest" and the MOF as the rigid framework, the enzymolysis efficiency of the nano-reactors was improved significantly because the confinement effect induced by the polymer chains formed a "soft nest" at high temperature. One of the proposed nano-reactors was further applied in monitoring of rat serum glucose. This study provides a new avenue for designing stimuli-responsive polymer–MOF based nano-reactors by considering the molecular weights or sizes of the enzymes and guiding them in practical application.

## Author contributions

L. Qi designed the study. J. Qiao and C. Cheng performed the experiments and data collection. J. Qiao and C. Cheng prepared the manuscript. L. Qi and D. Li revised the manuscript.

## Conflicts of interest

There are no conflicts of interest to declare.

## Acknowledgements

This work was supported by the National Natural Science Foundation of China (no. 22274159 and 22074148).

## Notes and references

1 A. Schmid, J. S. Dordick, B. Hauer, A. Kiener, M. Wubbolts and B. Witholt, Industrial biocatalysis today and tomorrow, *Nature*, 2001, **409**, 258–268.
2 S. Prasad and I. Roy, Converting enzymes into tools of industrial importance, *Recent Pat. Biotechnol.*, 2018, **12**, 33–56.
3 A. Kuchler, M. Yoshimoto, S. Luginbuhl, F. Mavelli and P. Walde, Enzymatic reactions in confined environments, *Nat. Nanotechnol.*, 2016, **11**, 409–420.
4 R. A. Sheldon and S. Van Pelt, Enzyme immobilisation in biocatalysis: Why, what and how, *Chem. Soc. Rev.*, 2013, **42**, 6223–6235.
5 X. Lian, Y. Fang, E. Joseph, Q. Wang, J. Li, S. Banerjee, C. Lollar, X. Wang and H. C. Zhou, Enzyme-MOF (metal–organic framework) composites, *Chem. Soc. Rev.*, 2017, **46**, 3386–3401.
6 P. Li, J. A. Modica, A. J. Howarth, L. E. Vargas, P. Z. Moghadam, R. Q. Snurr, M. Mrksich, J. T. Hupp and O. K. Farha, Toward design rules for enzyme immobilization in hierarchical mesoporous metal–organic frameworks, *Chem*, 2016, **1**, 154–169.
7 S. M. Huang, X. X. Kou, J. Shen, G. Chen and G. F. Ouyang, ''Armor-plating'' enzymes with metal–organic frameworks (MOFs), *Angew. Chem., Int. Ed.*, 2020, **59**, 8786–8798.
8 Y. Pan, H. Li, J. Farmakes, F. Xiao, B. Chen, S. Ma and Z. Yang, How do enzymes orient when trapped on metal–organic framework (MOF) surfaces, *J. Am. Chem. Soc.*, 2018, **140**, 16032–16036.
9 I. Gill and A. Ballesteros, Encapsulation of Biologicals within Silicate, Siloxane, and Hybrid Sol-Gel Polymers: An Efficient and Generic Approach, *J. Am. Chem. Soc.*, 1998, **120**, 8587–8598.
10 R. A. Sheldon, Enzyme Immobilization: The Quest for Optimum Performance, *Adv. Synth. Catal.*, 2007, **349**, 1289–1307.
11 E. S. Lee, M. J. Kwon, H. Lee and J. J. Kim, Stabilization of protein encapsulated in poly(lactide-*co*-glycolide) microspheres by novel viscous S/W/O/W method, *Int. J. Pharm.*, 2007, **331**, 27–37.
12 K. Y. Leea and S. H. Yuk, Polymeric protein delivery systems, *Prog. Polym. Sci.*, 2007, **32**, 669–697.
13 M. Hartmann and D. Jung, Biocatalysis with enzymes immobilized on mesoporous hosts: the status quo and future trends, *J. Mater. Chem.*, 2010, **20**, 844–857.
14 C. Doonan, R. Ricco, K. Liang, D. Bradshaw and P. Falcaro, Metal–Organic Frameworks at the Biointerface: Synthetic Strategies and Applications, *Acc. Chem. Res.*, 2017, **50**, 1423–1432.
15 H. C. Zhou and S. Kitagawa, Metal–Organic Frameworks (MOFs), *Chem. Soc. Rev.*, 2014, **43**, 5415–5418.
16 T. T. Man, C. X. Xu, X. Y. Liu, D. Li, C. K. Tsung, H. Pei, Y. Wan and L. Li, Hierarchically encapsulating enzymes with multi-shelled metal–organic frameworks for tandem biocatalytic reactions, *Nat. Commun.*, 2022, **13**, 305.
17 H. Shen, H. M. Shi, Y. Yang, J. Y. Song, C. F. Ding and S. N. Yu, Highly efficient synergistic biocatalysis driven by stably loaded enzymes within hierarchically porous iron/cobalt metal–organic framework *via* biomimetic mineralization, *J. Mater. Chem.*, 2022, **10**, 1553–1560.
18 S. Patra, T. Hidalgo Crespo, A. Permyakova, C. Sicard, C. Serre, A. Chaussé, N. Steunou and L. Legrand, Design of metal organic framework-enzyme based bioelectrodes as a novel and highly sensitive biosensing platform, *J. Mater. Chem. B*, 2015, **3**, 8983–8992.
19 Z. H. Zhao, Y. J. Huang, W. R. Liu, F. G. Ye and S. L. Zhao, Immobilized glucose oxidase on boronic acid-functionalized hierarchically porous MOF as an integrated nanozyme for one-step glucose detection, *ACS Sustainable Chem. Eng.*, 2020, **8**, 4481–4488.
20 J. Chen, B. Z. Sun, C. R. Sun, P. L. Zhang, W. F. Xu, Y. Liu, B. Q. Xiong and K. W. Tang, Immobilization of lipase AYS on UiO-66-$NH_2$ metal–organic framework nanoparticles as a recyclable biocatalyst for ester hydrolysis and kinetic resolution, *Sep. Purif. Technol.*, 2020, **251**, 117398.
21 X. Z. Lian, Y. P. Chen, T. F. Liu and H. C. Zhou, Coupling two enzymes into a tandem nanoreactor utilizing a hierarchically structured MOF, *Chem. Sci.*, 2016, **7**, 6969–6973.
22 G. S. Chen, X. X. Kou, S. M. Huang, L. J. Tong, Y. J. Shen, W. S. Zhu, F. Zhu and G. F. Ouyang, Modulating the biofunctionality of metal–organic-framework encapsulated enzymes through controllable embedding patterns, *Angew. Chem., Int. Ed.*, 2020, **59**, 2867–2874.
23 H. D. An, M. M. Li, J. Gao, Z. J. Zhang, S. Q. Ma and Y. Chen, Incorporation of biomolecules in metal–organic frameworks for advanced applications, *Coord. Chem. Rev.*, 2019, **384**, 90–106.
24 B. J. Johnson, W. R. Algar, A. P. Malanoski, M. G. Ancona and I. L. Medintz, Understanding enzymatic acceleration at nanoparticle interfaces: Approaches and challenges, *Nano Today*, 2014, **9**, 102–131.
25 L. Klermund and K. Castiglione, Polymersomes as nanoreactors for preparative biocatalytic applications: current challenges and future perspectives, *Bioprocess Biosyst. Eng.*, 2018, **41**, 1233–1246.
26 U. Hanefeld, L. Gardossi and E. Magner, Understanding Enzyme Immobilisation, *Chem. Soc. Rev.*, 2009, **38**, 453–468.
27 X. L. Wu, H. Yue, Y. Y. Zhang, X. Y. Gao, X. Y. Li, L. C. Wang, Y. F. Cao, M. Hou, H. X. An, L. Zhang, S. Li, J. Y. Ma, H. Lin, Y. N. Fu, H. K. Gu, W. Y. Lou, W. Wei, R. N. Zare and J. Ge, Packaging and delivering enzymes by amorphous metal–organic frameworks, *Nat. Commun.*, 2019, **10**, 5165.
28 H. D. An, J. Song, T. Wang, N. N. Xiao, Z. J. Zhang, P. Cheng, S. Q. Ma, H. Huang and Y. Chen, Metal–organic framework disintegrants: Enzyme preparation platforms with boosted activity, *Angew. Chem., Int. Ed.*, 2020, **59**, 16764–16769.
29 G. S. Chen, S. M. Huang, X. X. Kou, F. Zhu and G. F. Ouyang, Embedding functional biomacromolecules within peptide-

directed metal–organic framework (MOF) nanoarchitectures enables activity enhancement, *Angew. Chem., Int. Ed.*, 2020, **59**, 13947–13954.

30 Q. P. Wang, M. Chen, C. Xiong, X. F. Zhu, C. Chen, F. Y. Zhou, Y. Dong, Y. Wang, J. Xu, Y. M. Li, J. D. Liu, H. J. Zhang, B. J. Ye, H. Zhou and Y. Wu, Dual confinement of high-loading enzymes within metal–organic frameworks for glucose sensor with enhanced cascade biocatalysis, *Biosens. Bioelectron.*, 2022, **196**, 113695.

31 J. Qiao, J. F. Jiang, L. L. Liu, J. Shen and L. Qi, Enzyme reactor based on reversible pH controlled catalytic polymer porous membrane, *ACS Appl. Mater. Interfaces*, 2019, **11**, 15133–15140.

32 K. L. Heredia, D. Bontempo, T. Ly, J. T. Byers, S. Halstenberg and H. D. Maynard, *In Situ* Preparation of Protein-''Smart'' Polymer Conjugates with Retention of Bioactivity, *J. Am. Chem. Soc.*, 2005, **127**, 16955–16960.

33 J. Shen, J. Qiao, X. Y. Zhang and L. Qi, Dual-stimuli-responsive porous polymer enzyme reactor for tuning enzymolysis efficiency, *Microchim. Acta*, 2021, **188**, 435.

34 P. H. Tang, P. Berilyn So, K. R. Lee, Y. L. Lai, C. S. Lee and C. H. Lin, Metal organic framework-polyethersulfone composite membrane for iodine capture, *Polymers*, 2020, **12**, 2309.

35 H. Zhou, L. Dai, D. Liu and W. Du, MOF-derived hierarchically ordered porous carbon for the immobilization of Eversa® Transform 2.0 and its post-immobilization hydrophobization in biodiesel production, *Fuel*, 2023, **339**, 127426.

 